Back to Session Subjects

[1]AN ONBOARD WARNING SYSTEM TO PREVENT HAZARDOUS *"VORTEX RING STATE"* ENCOUNTERS

D. J. Varnes, R. W. Duren, and E. R. Wood
Department of Aeronautics and Astronautics
Naval Postgraduate School
Monterey, California
U.S.A.

1. Abstract

The aerodynamic phenomenon known as Vortex-Ring State (VRS) has long been recognized as the roughest regime of helicopter flight -- a condition of powered flight where the helicopter settles into its own downwash [Ref. 1]. As such it has always been considered a flight regime to be avoided when detected early enough. Severe thrust fluctuations, high vibration levels, sluggishness of control response that frequently leads to temporary loss of helicopter control, are typical characteristics associated with this dangerous and undesirable flight condition.

Data gathered from the U. S. Navy, the U. S. Army, the National Transportation Safety Board, and the Air Accidents Investigation Branch of the United Kingdom between 1982 and 1997 conservatively attribute Vortex-Ring State as causing at least 32 helicopter accidents in this time frame. Most of these accidents occurred at altitudes less than 200 feet at low airspeeds. In many instances application of collective control was not only ineffective in escaping Vortex-Ring State, but served to exacerbate the accident by increasing an already undesired rate of descent. It is significant that several of the mishap narratives state that Vortex-Ring State was unrecognized by the pilots.

The need for improved pilot aids has become a high priority item for pilots and aircrews operating at sea and ashore. Pilot aids such as moving map displays,

[1] Presented at 26th European Rotorcraft Forum, The Hague, The Netherlands, 26 to 29 September 2000.

collision, and now Vortex-Ring State (VRS) warning systems promise to significantly enhance aircrew situational awareness and safety. This paper discusses, examines and selects a Vortex-Ring State prediction algorithm to be incorporated in a PC-based onboard ground/air display tracking unit, known by the acronym GADGHT (Ground/Air Display for Geophysical/Hydrographic Tracking) [Ref. 2]. The onboard unit provides both an audible and visual warning to pilots once the aircraft has penetrated the Vortex-Ring State (VRS) boundary and by this means provides an extra margin of safety and situational awareness to helicopter crews operating in this type of dangerous flight environment.

2. Introduction

The impetus for development of an onboard warning system for Navy helicopters resulted from a two-phase study effort that focused on study of the "Vortex-Ring State Phenomenon". The first phase of the study was a survey of available accident data. The second phase explored the nature and seriousness of the phenomenon as revealed in published theoretical and experimental findings to date. Both these activities were conducted as part of a Naval Postgraduate School Master's degree program [Ref. 3] by LCDR David J. Varnes under the guidance of Professors Russell Duren and Bob Wood of the school's Department of Aeronautics and Astronautics.

For the accident survey, Data was gathered from the United States Navy, Marine Corps, Army, National Transportation Safety Board (NTSB), and the Air Accidents Investigation Branch (AAIB) from the United Kingdom. The search revealed 42 incidents causing accidents from 1982 through 1997. Four of these were attributed to Vortex-Ring State of the tail rotor. One of the accidents resulted in 11 fatalities. Several of the incident reports mention flight characteristics that are associated with Vortex-Ring State. These include aircraft vibrations, shudder, high rates of descent, and lack of response or negative response to the application of collective.

Although 42 incidents is a limited number of these events, the study revealed that Vortex-Ring State probably occurs on a much larger scale than these numbers indicate. The data collected only presents instances of Vortex-Ring State occurrence that have resulted in actual accidents or mishaps. Review of other reports strongly suggested Vortex-Ring State involvement, but did not specifically state it as a causal factor in the accidents. Additionally, informal discussions with pilots frequently prompted many of them to recall with great fervor instances in which they have encountered Vortex-Ring State and have successfully flown clear of it without damage to the helicopter or injury to the crew. Their claimed recovery from Vortex-Ring State ranged from almost immediate to a few hundred feet to several thousand feet. These instances frequently went unreported, and therefore, not discussed. Either embarrassment or a lack of appreciation for the potential consequences of Vortex-Ring State prevented these circumstances from being reported in an appropriate form. Furthermore, terminology inconsistency lends confusion to properly understanding and researching Vortex-Ring State. For example, settling with power and power settling will have opposite connotations depending on whom you may talk with. Civilian and Army helicopter pilots as well as some of the academic community will refer to Vortex-Ring State as settling with power, whereas the Naval Aviator and other academia will refer to this phenomenon as power settling.

It became apparent that there was not only confusion over the various terms used synonymously with Vortex-Ring State, but widespread misunderstanding of the fundamental nature of Vortex-Ring State and power settling – as defined by the NTSB and Army. Though power settling may certainly precipitate Vortex-Ring State

they are two distinctly different phenomena requiring dissimilar recovery techniques. This misunderstanding points to a lack of training and awareness, which are crucial to either phenomenon's prevention. An excellent article appearing in the May 1999 edition of *Rotor & Wing,* titled "Dead Air," written by Mr. Benjamin Moore addressed the misconceptions that abound between the two phenomena [Ref. 4]. His article stressed proper preflight mission planning as well as heightened awareness of the performance limitations of one's helicopter as key to avoiding disaster. While this is particularly true for situations of power settling, it does not necessarily assure that one will forestall Vortex-Ring State. The best flight planning cannot prevent an engine failure or the possible rate of descent incurred because of such a failure. This critical distinction furnished the impetus for the development of a Vortex-Ring State warning system to provide the pilot added safety and elevated awareness of the Vortex-Ring State boundary. Also, with the onset of increasingly demanding helicopter missions in less than ideal environments, the occurrence of Vortex-Ring State is likely to become more frequent.

Further contributing to confusion about the phenomenon is the fact gleaned from the H-34 flight test data studied for this review [Ref. 5] that VRS shows itself to be a dual valued phenomenon. That is, it was found from test data that within the Vortex-Ring State descent range, it is possible at a given rate of descent to obtain two equilibrium VRS states at a given descent rate at two different collective pitch settings corresponding to two different power settings. Further, associated with each power setting, blade airload measurements show totally different radial distributions of blade airload distribution, each with its own characteristic time history, as would be expected for a dual-valued flow condition. See Figures S-1 through S-8 and accompanying discussion presented in Section 7. of this paper.

3. Vortex Ring State Flow Field Defined

The easiest way to understand the Vortex-Ring State is to first consider the three basic flow states that exist for the rotor in purely vertical flight. These are the (1) *normal working state,* (2) *the Vortex-Ring State and* (3) *windmill brake state.* The flow conditions of these states are graphically illustrated in Figure 1 (from [Ref. 6]).

The normal working state according to [Ref. 7.] may be defined as the state wherein air approaches the rotor in the same direction as the induced velocity. The flow is downward through the disk and the flow at the disk is always equal to or greater than the induced velocity. The normal working state includes conditions from infinite rate of climb to hovering. Flight test results of [Ref. 5] and the theory of Gao-Xin [Ref. 8] indicate this range extends further possibly into the rate of descent range to about 25% of the induced velocity value.

In the normal working state the average hover induced velocity can readily be shown by momentum theory to be given by the classical expression:

$$V_H = \sqrt{\frac{T}{2\rho A}}$$

where, T is the thrust of the rotor, A is the area of the rotor disk, and Δ is density of air.

The purist considers the rotor to have entered Vortex-Ring State in vertical flight as soon as the rotor starts to descend from hover. We find in this case that the resultant flow through the disk is still downward because of the large induced velocity, but the flow far above the rotor is upward. The classical upper and lower bounds of the Vortex-Ring State are hovering flight and the condition where the rate of descent is equal to twice the average induced velocity at the rotor.

The Vortex-Ring State is characterized by the absence of a definite slipstream and large recirculating flows. The characteristics of this flight regime do not

lend themselves to treatment by classical momentum theory. Another way of considering VRS is to recognize that the center of the range encompasses the condition where the rotor is descending at the same rate of descent as its induced velocity. At this condition, the rotor's wake is no longer transported away by the flow of the rotor but instead the blades must repeatedly move through vortices previously shed by earlier blade passes. This accounts for the large impulsive loading imparted to the blades and the resulting high vibration levels characterized by this flow regime.

The Windmill-brake State (the VRS lower bound) occurs at large rates of descent where the flow again becomes smooth and a definite slipstream once more exists. Here, the flow is up through the rotor and its velocity decreases as the flow approaches and passes through the rotor as a result of the induced velocity, which opposes the direction of motion of the main flow. The slipstream thus expands smoothly above the rotor and the flow can once again be treated by momentum theory.

Summarizing our description of the rotor flow field (in vertical flight), there are three distinct flow regimes. These are (1) Normal working state; (2) Vortex-Ring State; and (3) Windmill-brake State. The boundaries between these flow regimes in vertical flight, in turn, establish the upper and lower bounds for the Vortex-Ring State. In vertical flight these values were initially taken as: (1) Between hover and any perceivable descent rate set the upper bound of the Vortex-Ring State; and (2) The lower bound of the Vortex-Ring State occurred at a vertical rate of descent equivalent to twice the average momentum value of hover induced velocity. The symbol for hover induced velocity is typically given as either V_H or V_i.

3.1 Vortex-Ring State Boundary Extended to Cover Flight Envelope

As the helicopter increases its forward velocity, the boundaries for the VRS envelope change from those of pure vertical flight. See Figures 3 through 6. A discussion of how the boundary was determined for the warning system is given in Section 6 of the paper. The algorithm selected for plotting the VRS boundary was chosen based on research performed by LCDR David Varnes [Ref. 3]. The algorithm was chosen based on an analysis of three previous prediction algorithms and on comparisons with NASA flight test data of an H-34 helicopter [Ref. 5]. Other work described in his thesis includes an analysis of the terminology associated with the Vortex-Ring State, a survey of relevant safety data, and a quick look at secondary indicators of the Vortex-Ring State.

4. Description of Vortex-Ring State Pilot Warning System

Helicopter pilots are trained to avoid the Vortex-Ring State by controlling their rate-of-descent. However the safety data reveals that this training does not always prevent entry into the Vortex-Ring State. Vortex-Ring State is typically entered as a result of a loss of situational awareness. Significant numbers of the accidents were the result of accepting slight tailwinds or downwind approaches reducing the actual horizontal air velocity. Unfortunately, the airspeed indication on most helicopters is ineffective below 35 to 40 knots. Another typical scenario involved steep descents from high hovers. In these situations, the vertical descent rate can increase with less visual feedback to indicate potential trouble. Once, Vortex-Ring State had been entered, it was often misinterpreted. In some instances incorrect pilot identification of Vortex-Ring State led to control inputs that further exacerbated the situation. Though Vortex-Ring State is not an everyday occurrence, today's modern helicopter and its broad spectrum of missions dictate operations in an environment where the occurrence of either Vortex-Ring State or settling with power are increasingly likely.

As a result of this research, it was determined that it would be beneficial to

develop a system to enhance aircrew situational awareness and safety by providing pilots adequate warning of the potential existence of Vortex-Ring State. This warning would ensure accurate identification of the current flight condition and permit subsequent correct recovery procedures to be made with confidence and without delay preventing mishaps and accidents. The idea is similar to that behind ground proximity warning systems (GPWS). CFIT, or controlled flight into terrain, is another type of accident that results from the loss of situational awareness. A GPWS alerts the pilot when he is approaching a boundary with terrain. The Vortex-Ring State warning system alerts the pilot when he is approaching a unsafe boundary in the flight envelope. It should be noted that a system that is used to provide a VRS warning has other benefits. Since it is keeping track of the aircraft's position within the flight envelope it can also be used to indicate other boundaries of the flight envelope, such as the dead man's curve, etc.

Conceptually, the warning system is relatively easy to understand. The Vortex-Ring State boundary is a function of airspeed, hover-induced velocity, and rate of descent. Hover induced velocity is a function of weight and air density. If you can measure these parameters (which is possible with the correct instrumentation) then you can develop a warning. The key avionics requirement for the system is accurate low airspeed data. Multiple systems and techniques exist for developing true airspeed. These are beyond the scope of this paper.

Working in conjunction with the NAWCAD VH Systems Engineering Integrated Product Team a Vortex-Ring State Warning System has been developed and successfully demonstrated. Plans originally called for demonstrating the warning system on a CH-60 helicopter at Patuxent River. Delays in delivery of the helicopter required the development of a simulation of the CH-60 avionics system. A portable personal computer was equipped with a multi-channel ARINC 429 transceiver and a graphical user interface (GUI) was developed to simulate the helicopter. The aircraft simulator user interface shown in Figure 1 allows the user to specify fuel weights, static air temperature, static pressure, altitude rate,

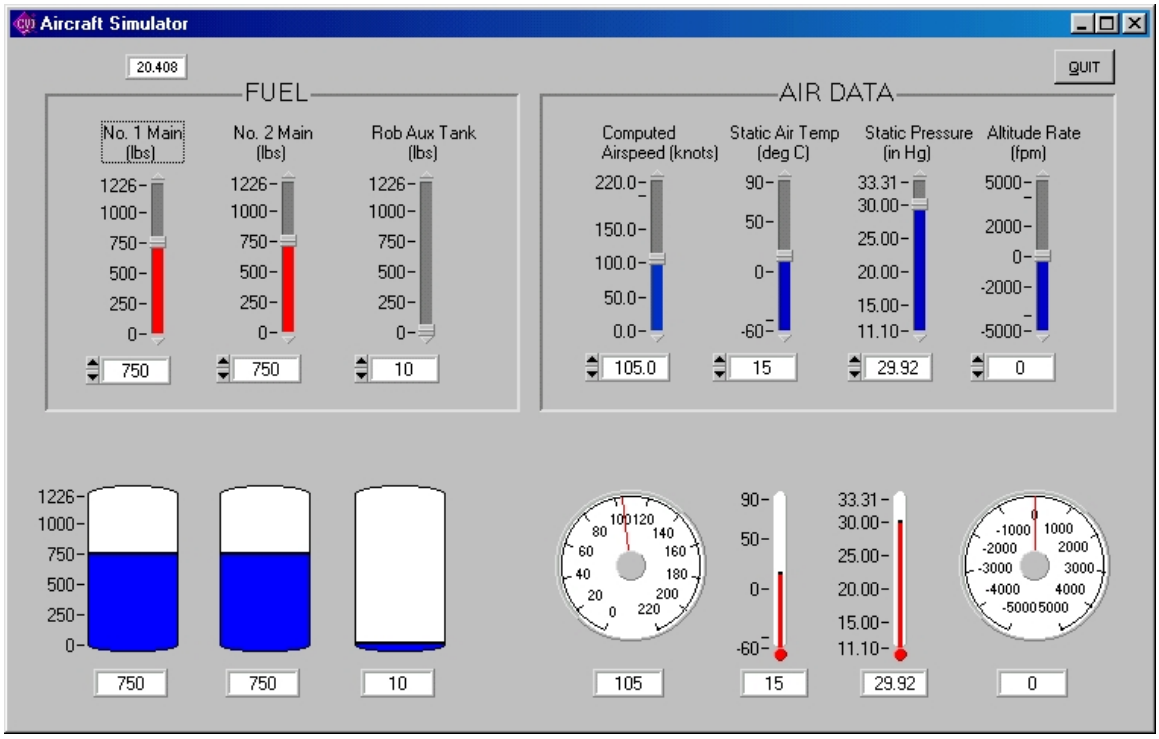

Figure 1. Aircraft Simulator

and airspeed. The upper half of the aircraft simulator GUI allows the user to enter the data. Data is sent out over two ARINC 429 buses at the same data rates as on the actual helicopter. Below the GUI input area is a display area that shows the data taken from the appropriate receive channel of the ARINC 429 card. This was instrumental in showing that the data supplied by the user was converted to correct ARINC 429 format and pulled off the ARINC 429 receive channel just as would be done in an actual aircraft implementation. A lunchbox computer housed the ARINC 429 card as well as the Windows-based simulation software.

The Vortex-Ring State (VRS) Monitor was also implemented as a Windows program. It is intended to be run in conjunction with other programs including FalconView moving map software on the GADGHT kneeboard computer system. The VRS program allows the user to select a helicopter type and enter a base weight. The choice of a helicopter type automatically sets the rotor radius, used to calculate the hover induced velocity, and the information necessary to pull required data, such as air data and fuel quantity, from whatever avionics configuration (MIL-STD 1553 or ARINC-429) exists on that type of helicopter. The base weight is the helicopter's weight including crew and equipment, but without fuel weight. The VRS program currently defaults to a CH-60 and a base weight of 18,000 pounds. If a base weight other than 18,000 pounds is desired the user simply clicks on the base weight display window to bring up a numeric keypad in order to make a different entry. Clear and Enter keys are also available on the keypad. Once 'ENT" has been selected the keypad will close and the entered weight will be displayed. Data monitored over an ARINC-429 data bus provides real time updates of the fuel weight for each tank used in the helicopter. Once the helicopter type and base weight have been set, the user may select 'RUN' for the application to begin. Figure 2 shows the VRS GUI during the process of updating the base weight.

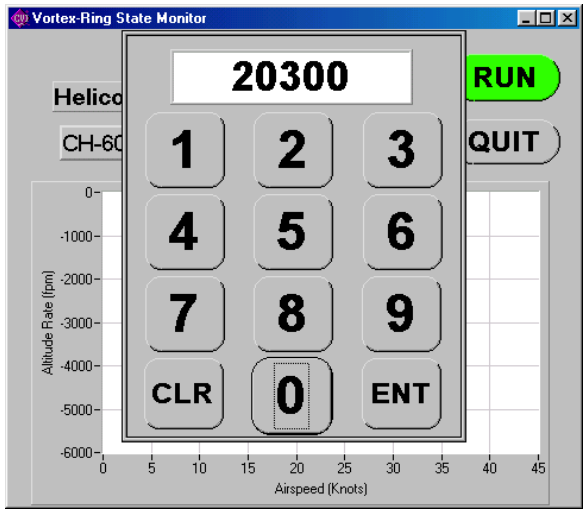

Figure 2. Entering Base Weight

When the 'RUN' button is activated, the VRS program computes a boundary based on the current atmospheric conditions and helicopter weight. This boundary is plotted on a graph on the VRS display. The helicopter's position in terms of airspeed and rate of descent is shown on the graph with a helicopter icon. Any value outside of the range of the graph is defaulted to the maximum value appearing on the graph. Thus, there is no confusion from what direction the helicopter is approaching the Vortex-Ring State boundary. The VRS display can be minimized allowing other applications to be used. Penetration of the Vortex-Ring State boundary causes the VRS display to maximize itself, covering all other applications. Simultaneously, the program begins flashing the background color surrounding the graph and issues an aural warning. The aural warning is recorded as a .wav file. For the demonstration it was played on speakers. In the aircraft it will be sent to the pilot over the intercom system. The program will not allow minimization of the main window while a penetration of the Vortex-Ring State boundary exists. Should the weight of the helicopter need to be updated, i.e., additional passengers, a 'STOP' button may be depressed in order to allow the base

weight to be changed. The program may minimized while not in a warning by selecting the 'HIDE' button or closed completely by depressing the 'QUIT' button.

Figures 3 through 6 illustrate the operation of the VRS program. Figure 3 shows the helicopter in level flight at a speed of 105 knots. The helicopter icon is shown partially off screen at the upper right-hand corner of the graph. The vortex-ring boundary is shown for standard atmospheric conditions and a base weight of 18,000 pounds. Figure 4 shows a similar display where the atmospheric conditions and helicopter weight have increased the required hover induced velocity. This results in a VRS boundary that is shifted down on the graph and increased in size. Figure 5 shows a helicopter during a safe descent. The helicopter has an airspeed of 35 knots and is descending at a rate of 2000 fpm. Figure 6 shows a helicopter that has penetrated the VRS boundary causing a warning to be issued.

The kneeboard computer system that hosts the VRS warning program was developed by the VH Systems Engineering IPT. It is connected to the aircraft's avionics data buses as a bus monitor or receiver. The installation requires no modification to existing avionics

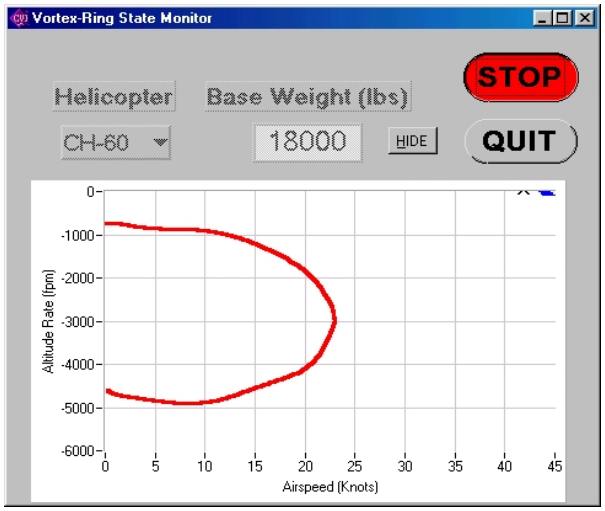

Figure 3. Level Flight on a Standard Day

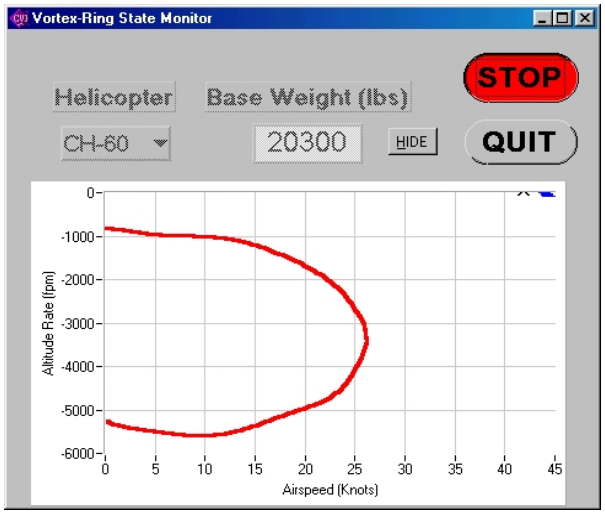

Figure 4. Level Flight, Hot and Heavy

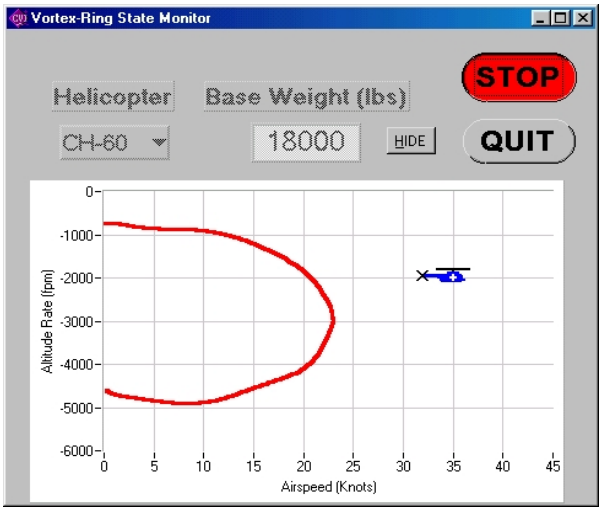

Figure 5. Performing a Safe Descent

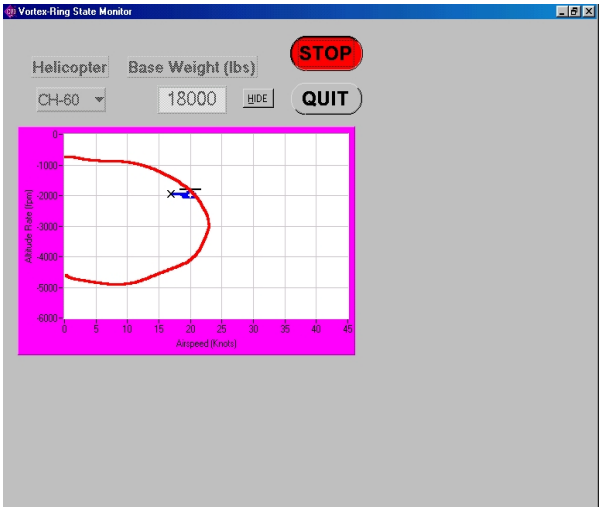

Figure 6. Maximized Display while Issuing Warning

operational flight programs (OFPs). This allows new functions to be added quickly without disturbing existing systems. The next step in the development of the VRS Warning System will be to verify the operation of the complete system on an actual aircraft. This will be followed by flight testing to validate the boundary calculated by the prediction algorithm. Plans are being developed to accomplish flight testing in the near future.

5. Vortex-Ring State Boundary Prediction Algorithms

Three different theories for Vortex-Ring State boundary prediction were examined for use in the NPS Vortex-Ring State warning system. The theories were reviewed for several attributes including the use of wind tunnel testing in support of conclusions, conformity to known flight test data, and their adaptability for use in the warning system implementation. This review is discussed in detail in LT David Varnes thesis [Ref. 3]. A description of the development of these theories will now be given.

5.1 Wolkovitch

The most commonly referenced Vortex-Ring State prediction algorithm is that of Dr. Julian Wolkovitch. He presented the algorithm in a paper published in the *Journal of the American Helicopter Societ*y, in July, 1972 titled, "Analytical Prediction of Vortex-Ring State Boundaries for Helicopters in Steep Descents." [Ref. 9]. This article appears to be one of the first theories published that made an attempt to utilize momentum theory in combination with empirical data to predict the location of the Vortex-Ring State boundary.

The boundary is typically given as a closed line figure on plot of the helicopter's rate of descent in feet per minute versus the aircraft's speed in knots. Wolkovitch's motivation for better defining the Vortex-Ring State boundaries was twofold. First, was the requirement to design helicopters that could perform steep descents with normal engine functioning. Second, knowing the Vortex-Ring State boundaries was important for ensuring that a twin engine helicopter experiencing a single engine failure could safely descend.

5.2 Peters and Chen

Another commonly referenced source for Vortex-Ring State prediction is that of Dr. David Peters and Shyi-Yaung Chen. Their paper was published in the *Journal of the American Helicopter Society* in July 1982, [Ref. 10]. Peters' and Chen's motivation for conducting their study was to reexamine Vortex-Ring State boundary prediction criteria, as presented by Wolkovitch, and to extend the criteria to include a more consistent wake model. Peters and Chen introduce their discussion by defining the helicopter normal working state, windmill brake state, and the Vortex-Ring State. They consider the helicopter state to be that flight condition where the rotor is imparting energy to the flow field via the induced flow. In the Windmill State the rotor is extracting energy from the air by slowing the freestream. Vortex-Ring State is defined to be the region in which the concept of a momentum supported slipstream is no longer valid, which, can include both the helicopter and windmill state. This is an important point to keep in mind when the Vortex-Ring State boundary is presented. [Ref. 10]

a. Background

Peters and Chen begin their study by reexamining momentum theory as it applies to rotors in yawed flow. Yawed flow is a term used to indicate that an inplane component of velocity exists. One could also describe this inplane component as either the horizontal component of velocity that the helicopter generates as it moves forward, or the horizontal velocity component of the wind it experiences, or both. They continue their discussion by deriving an equation that relates the normalized rate of descent h, horizontal velocity m, and induced flow n.

b. Upper And Lower Boundary

One of the main criticisms of Wolkovitch leveled by Peters and Chen is that the earlier theory does not take into account a wake propagation angle. Instead, Wolkovitch's flow model assumes the flow to propagate directly down. There would appear to be no maximum inplane velocity at which Vortex-Ring State does not occur. This is not consistent with experimental or actual flight test data. In fact, one of the primary methods often discussed for escaping Vortex-Ring State is an application of forward cyclic to increase the airspeed. This velocity is the same as an increase in the inplane velocity component, thus sweeping the unsteady flow behind the helicopter. Therefore, Peters and Chen suggest a new flow model and boundary, that accounts for the propagation angle of the wake due to an inplane velocity component.

c. Concluding Remarks

The following remarks can be made concerning the Peters and Chen Vortex-Ring State boundary:

- Peters and Chen show no existence of Vortex-Ring State above a normalized or inplane velocity component of 0.62.
- Vortex-Ring State can occur over a wider range of rates of descent.
- The center, not the edge, of the Vortex-Ring State region is considered to be the point at which the normalized rate of descent is equal to 0.707.

5.3 Gao and Xin

Professor Zheng Gao and his graduate student Hong Xin, both from the Institute of Helicopter Technology-Nanjing University of Aeronautics & Astronautics, published a paper in 1994 in the First Russian Helicopter Society Annual Forum Proceedings entitled, "An Experimental Investigation on Vortex-Ring State Boundary" [Ref. 8]. A motivating factor cited by the authors, for researching this problem were the numerous helicopter accidents in China attributed to Vortex-Ring State. The lack of existing satisfactory methods for determining the Vortex-Ring State boundaries prompted Gao and Xin to take a more experimental approach to solving this dilemma.

a. Experimental Set Up

It was essential that if a Vortex-Ring State boundary was to be obtained experimentally the test apparatus used in the study must be highly reliable and free of common wind tunnel testing limitations. With this in mind, Gao and Xin developed a test apparatus free from two main limitations associated with the typical wind tunnel. The first wind tunnel limitation is that it is difficult to account for the severe interference effects from the wind tunnel wall because of the size of the fluctuating air body around the rotor system, which can extend to a distance of several rotor diameters in the Vortex-Ring State. Second, many wind tunnels demonstrate poor low speed characteristics in the low speed region required to study Vortex-Ring State. Gao and Xin developed a six-meter long whirling beam mounted with a model rotor driven by an a/c. electric motor and attached to a scaled model fuselage of a Bell 206. The model rotor had the ability to be fixed on the beam in several radial locations.

Additionally, level, vertical and oblique flight conditions were modeled by changing the orientation of the axis of the model rotor. The whirling beam could be adjusted to rotate anywhere from 0 to 30 rpm allowing several descent velocities to be examined. Three sets of rotor blades with varying characteristics were utilized in the experimental studies.

The function of the whirling beam was to measure the torque and thrust experienced by the rotor system. This was accomplished with the use of a strain-gauge balance system located between the motor and the hub of the rotor. Four leaf springs were used to sense the thrust, and a torsion tube was used to gather the torque data.

After passing through an amplifier the signals were sent to a computer where they were sampled and converted to digital data to be graphed as output. [Ref. 8]

b. Testing and Reduction of Data

Fourteen groups of tests were conducted using various blade sets . The model rotor was fixed on the whirling beam at a radial location of five meters. For each testing group the rotational speed of the whirling beam was increased incrementally at each testing point. The first and last testing points of each group were for hovering conditions. Gao and Xin point out that at each test point the rotor was not started until the beam had been adjusted to rotate steadily at the desired speed. Once this stability was achieved data points were then sampled and the time histories of the torque and thrust were recorded. Sampling was also completed before and after the rotor was engaged while the whirling beam was rotating in order to obtain the fore and aft zeroes of the measurements at that test point. The zero drifts of each channel were monitored by checking the repeatability of the fore and aft zeroes of each test point as well as the first and last hovering values of the test group. [Ref. 8]

For each test point, the average value of the pair of fore and aft zeroes was used as the mean zero and subtracted from the sampled data when the rotor was running. Furthermore, the data was averaged over the sampling period in order to obtain mean values at that particular velocity. [Ref. 8].

Gao and Xin eliminated centrifugal force effects by subtracting the zeroes that were measured, as described before, when the beam was rotating. Other sources of error included a flapping motion of the rotor blades that was introduced as a result of inplane component of the freestream velocity as well as a Coriolis moment acting on the rotor blades. This Coriolis moment resulted from the rotor axis not being parallel with the central pillar. Both of these errors were analyzed and expressed in terms of tilt angle errors of the rotor system. Because of the tilt angle errors, the measured thrust was slightly less than the actual value. A thrust correction was applied.

c. ***Results***

Gao and Xin discovered, like Wolkovitch, that the most severe region of the Vortex-Ring State in a vertical descent was the region in which the descent velocity was 0.6 to 0.8 of the rotor-induced velocity. ($0.6\ v_h < V < 0.8 v_h$).

Gao and Xin also determined that, according to their power spectra that the period of the aerodynamic fluctuations was approximately one to two seconds; the same as had been reported earlier by Drees, etc. who produced smoke study films in Holland in the late 1940's [Ref. 11].

One of the most significant findings highlighted by Gao and Xin was the correlation of their mean torque data to what many call the power settling phenomena of Vortex-Ring State. This phenomenon is, again, described as the situation where an increase in torque is observed for increasing descent velocity. In this region pilots find that an increase in collective is required even though they are in a descent. As can be seen from Figure 35, the mean torque is a minimum at a low descent velocity of about $V=0.28\ v_h$. Beyond this point the trend for the mean torque begins to rise and comes fairly close to leveling off at a descent velocity of $V=0.8\ v_h$. Beyond this point the mean torque rises again. Gao and Xin speculate that this second increase is due to local blade stall. After $V=0.8\ v_h$ torque fluctuations, however, gradually decrease as the rotor moves towards the windmill brake state.

The point at which the mean torque begins to increase with an increasing descent rate is defined by Gao and Xin to be the critical descent velocity. In other words, the value for which this power-settling region begins varies from 0.28 for the vertical descent to 0.55 for a descent angle of 45 degrees. Descent angles shallower

than 40 degrees do not indicate a mean torque behavior of this sort. Additionally, no evidence of the Vortex-Ring State was found for angles of descent less than 30 degrees. Therefore, Gao and Xin conclude that Vortex-Ring State cannot be entered for descent angles less than 40 degrees. Another interesting result reported by Gao and Xin was that for angles of descent between 60 and 75 degrees, the torque and thrust fluctuations are greater than those for the vertical descent are. This would indicate that the turbulence associated with the Vortex-Ring State is the highest when the descent angle is between 60 and 75 degrees.

6. VRS as Revealed by NASA H-34 Flight Test Data

In 1964, NASA Langley Research Center conducted an extensive flight test program to obtain rotor blade airloads, bending moments, and blade motions as well as to measure numerous flight parameters. The purpose of the program was to provide real-world experimental data on helicopter vibratory loads that was considered as lacking at that time. The tabulated data were presented without analysis in NASA Technical Memorandum X-952 by James Scheiman [Ref. 5]. Data was collected for forward flights from 0-120 knots, flights in and out of ground effect, climbs, autorotations, maneuvers, and operations with fore and aft center of gravity locations. This data was obtained through the instrumentation of a U.S. Army Sikorsky H-34.

More than 132 different flight conditions were flown of which more than 30 were partial power descents. Airloads were recorded at seven blade stations in 15-degree blade azimuth intervals. The most outboard blade station was at r/R of 0.95 with the most inboard blade station located at r/R 0f 0.25. The airload at each blade station was the integrated total of 7 chordwise pressure taps. In addtion, the blade was instrumented to record blade flapwise bending at 7 radial locations, blade chordwise bending at 5 radial locations and blade torsion at 2 blade radial positions.

Of particular interest to this study was the partial power descent flight tests and the corresponding pilot remarks. Partial power descent data was obtained for flight test numbers 55-76. Descents were initiated at airspeeds ranging from 0 to 113 knots. Actual descent rates varied from 0 to 2,600 feet per minute. The testing gross weight of the helicopter was reported to be between 11,200 and 11,805 lb. For calculations used in the Vortex-Ring State boundary determination an average weight of 11,502.5 lb. was used. Similarly, the air density for the partial power descent data varied from 0.00208 to 0.00244 slugs/cu ft . Averaging all of the reported air densities yielded a value of 0.00216 slugs/cu ft .

The H-34 was powered by a nine cylinder Curtis-Wright radial reciprocating engine. It had a 4-bladed articulated rotor of 56-ft diameter. Blade chord was 16.4 inches. Rotor rotational speed was nominally 212 rpm. Rotor offset was 12 inches. Rotor disk loading was 4.75 psf with a solidity of 0.0622 and a hover $C_T/\Phi = 0.0817$. Flapping and lag hinge offset was coincident at r/R = 12 inches. For the H-34, hover average induced velocity was $v_h = 1880$ fpm.

6.1 Partial Power Descents for H-34 in Vertical Flight

Shown in Figure 7 are the data points considered for the case where the H-34 is in partial power descent. Each point shown represents a flight test data point for which extensive flight test data was available from Ref. (S). Superimposed on the plot is the VRS envelope as defined by the Gao Xin theory. We should note several features of the diagram. For the H-34 tested, v_H = 1850 feet per minute. This occurs approximately in the center of the Gao-Xin envelope. Second, the bottom of the Gao-Xin envelope is at approximately 3700 fpm which is equivalent to the 2 v_H value specified by most theories and marks the entry velocity into vertical autorotation.

The Gao-Xin envelope is bounded by a maximum forward horizontal speed of about 20 knots. Also observe the relative high-speed descent points at horizontal velocities of about 68 knots and in the region from 105 to 120 knots. These data points were flight test points flown during the NASA-Army flight test program. They were not intentional partial power descent points. They were listed in the "Table of Contents" as "Trim Level Flight Out of Ground Effect". However, while not significant in the present study thy do represent high-speed points at one extreme part of the powered descent envelope, where horizontal speed is high and rate of descent is low.

Table I is a tabulation of all the flight test data points covered in Figure 7. Given is information including, "Flight Number", "Rate of Descent", "Approximate Forward Speed in Knots", "Manifold Pressure in Inches of Mercury", "Air Density", " Main Rotor N_R in rpm" and pilot remarks.

For the test program, the H-34 had an instrumented rotor blade that recorded spanwise blade airloads at 15-degree azimuth intervals for seven blade radial stations located at blade spanwise locations of r/R = 0.95, r/R = 0.85, r/R = 0.75, r/R = 0.55, r/R = 0.40, and r/R = 0.25, respectively. Spanwise airloads were obtained at each blade spanwise location by chordwise integration of seven differential pressure pickups at the following chord stations, taken from blade leading edge to trailing edge: x/c = 0.017, 0.040, 0.090, 0.130, 0.168, 0.233, 0.335, 0.500, 0.625, 0.769, and 0.915.

An indication of the relative change in impulsive loading of blade airloads per rotor revolution with change in descent rate can be evaluated by study of Figures 9 and 10. Shown on each of the two figures is the spanwise load time history as measured near the blade tip (r/R = 0.95) for different vertical descent rates at essentially zero forward velocity. The trace at the top of Figure 9 is the time history of blade loading at r/R = .95 for the rotor hovering out of ground effect. We note that for hover at this spanwise station, blade airload remains essentially constant at 32 lbs per running inch of blade span, with one exception. That is, the lift drops to about 22 lbs per inch of blade span each time the blade passes near the tail rotor, which is located at about $\Theta = 0^\circ$ azimuth interval or close to directly over the tailboom of the helicopter. In the center plot of Figure 9, the helicopter is descending at about 1000 fpm. We find the lift at the outboard blade station is down to about half its hover value, as is the engine manifold pressure. Airload time history shows only moderate impulsiveness. In contrast, in the case of the bottom plot of Fig. 9 we are clearly in VRS. Manifold pressure has increased by 80 percent over the power required at 1000 fpm and blade loading has become more impulsive. The situation is even more aggravated in the top two figures of Figure 10 where power now exceeds the HOGE value and the airloads have become extremely impulsive or choppy. At both these descent rates, pilot remarks are that the helicopter is temporarily out of control. In our last plot of Figure 10 we are at a descent rate of 2600 fpm and clearly still in VRS. Airloads are slightly improved over the previous two cases and power has backed off by about 10 percent.

Further insight into Figures 9 and 10 can be obtained by study of Figure 8. Here, engine power as measured by engine manifold pressure is plotted versus rate of descent for the H-34 in vertical descent. The plot shows several trends. We note that at the low rates of descent, less than 1000 fpm there is a gradual drop off in power with increase in rate of descent. This would be expected. Then at rates of descent above 1000 fpm there is a noticeable increase in engine power achieving a maximum power level where $v_D = v_{H.}$ Above this value (1850 fpm) engine power again drops off gradually diminishing as rate of descent approaches $2v_{H.}$

We also notice an anomaly for the data plotted in Figure 8. We observe that engine

power is dual valued at several discrete descent rates. That is, at a descent rate of about 950 fpm, two different flow regimes are established for the rotor, one for a power setting of 19.4 in. Hg., the other for a power setting of 33.5 in. Hg. We observe the same phenomenon at 1825 fpm. In one case a sustained descent rate of 1825 fpm is achieved with a power setting of 16.5 in. Hg., while in the other case the same sustained descent rate of 1825 fpm is achieved at a value of more than twice the power required for the other case, that of 40.1 in. Hg.

Figures 11 and 12 are presented in an effort to give the reader some understanding of what is contributing to these substantial differences in power setting, while yielding the same descent rate. Plotted in Figure 11 is a comparison between the blade lift distribution for the two power cases at a 950 fpm descent rate. Plots are given for every 45 degrees of blade azimuth interval. Figure 12 gives a similar comparison, but for the 1825 fpm descent rate.

Consider the upper right hand plot in Figure 11. What is shown is the lift distribution from root to tip of the blade for $\Theta = 0$ degrees azimuth position. This is the position where the blade is pointed aft. For the plot, the dashed line represents the lift distribution for a 950 fpm descent rate (power setting of 19.4 in. Hg.) whereas the solid line represents the same descent rate (950 fpm) but in this case the power is much higher (33.5 in. Hg.). The upper left diagram represents a plot similar to the one just described, except in the case the rotor blade is at $\Theta = 180$ degrees or directly over the nose of the helicopter.

For the second diagram down (of the four on the page) the right diagram gives the respective pressure or lift distribution at 950 fpm for the two power settings (19.4 in. Hg. and 33.5 in. Hg.) except in this case the blade has advanced to $\Theta = 45$ degrees counterclockwise as seen from above) from the case directly above it, which is at $\Theta = 0$ degrees. The lift distributions shown 2nd down, left hand page represent $\Theta = 225$ degrees, which is advanced 45 degrees from the blade case ($\Theta = 180$ degrees) that is at the top left position on the page, etc.

For the third blade pair down the page we have the respective lift distributions 45 degrees later with the advancing blade (right side of page) now located at $\Theta = 90$ degrees and the retreating blade (left side) now located to the left at $\Theta = 270$ degrees. The last pair of plots on the page for Figure 11 has the blade positioned at $\Theta = 135$ degrees on the advancing side (right) and the retreating blade (left) positioned at $\Theta = 315$ degrees. Were a fifth plot to be presented the advancing blade would have moved to the $\Theta = 180$ degree position and the retreating blade would one more occupy the $\Theta = 0$ degree location.

In summary we observe that Figure 11 gives us a comparison of the lift distribution acting over the rotor disk as depicted every 45 degrees of blade position. The case shown is partial power descent at 950 fpm and lift distributions are displayed for two steady-state power settings, one at 33.5 in. Hg. (high power), the other at 19.4 in. Hg. (low power). Comparing the lift distributions for the two power settings we observe the following:

- Higher power case has load shifted more outboard on blade.
- Lower power case has considerably smoother load distribution indicative of more even spanwise distribution of trailing vorticity.
- Tip vortex for high power case is stronger than low power case based upon gradient of blade bound circulation in tip region.
- For high power case, azimuthal variation of lift distribution with time appears more severe than low power case, indicating rougher, more impulsive blade loading in high power case.

Shown in Figure 12 is a similar comparison of blade radial distribution of lift for two steady-state power conditions (40.1 in. Hg. and 16.5 in. Hg.). The

horizontal velocity of the helicopter is essentially zero. The rate of descent in this case is 1825 fpm, or approximately v_H for the H-34. The trends noted in comparing the high power case to the low power case are similar to the findings with respect to Figure 11. There is one noticeable difference, which is that the outboard shift of blade loads for the high power case is not as pronounced here as in Figure 11.

Presented in Figure 13 are measured airloads from the NASA H-34 flight test program for four cases of trim and level flight. These airloads are presented so the reader can compare them with VRS airloads to get a comparison between normally experienced flight measured levels and those encountered in VRS. Given in Fig. 13 are flight measured values at r/R = 0.95 for hover O.G.E., for 42 knots level flight, for 68 knots level flight and for 112 knots level flight.

The smoothest levels are those shown for hover O.G. E. as might be expected. It is interesting to observe that tail rotor interference produces some moderate modulation of the hover airloads.

The roughest airloads are those at r/R = 0.95 at 42 knots. This is due to the very discernible cases of BVI occurring at about Θ = 90 degs. and at about 270 degs. and giving rise to the characteristic buildup in vibration levels generally noted in transition in the 40-knot airspeed region.

The modulation in airloads due to cyclic pitch is very mild at 68 knots which is the bottom of the bucket for the power required curve.

At 112 knots, we begin to see a buildup in the airload modulation due to the increased cyclic pitch requirements, but note that this modulation is low when contrasted with some of the plots obtained for the H-34 in partial power descent.

Fig. 14 shows a 3D representation of the roughness of actual airloads encountered during VRS. These are not the highest encountered since the rate of descent is above $V_{H.}$, but they do represent typical VRS vibratory airloads.

7. Acknowledgements

The demonstration and development of the new helicopter VRS Warning System could not have been completed without the assistance of many people. The ONR NSAP program provided funding and support for the development. Mr. Herman Kolwey from Pax River suggested the Vortex-Ring State problem and provided continuous technical assistance. Members of the VH Systems Engineering IPT were of great assistance in co-developing the two demonstration programs and configuring the hardware for the demonstration. In particular the efforts of Mr. Carl Zaslow and Mr. Jim Tomasic were indispensable. We are grateful to Mr. Erik Danielson, mechanical engineering student at UCSD, for his support with the text and graphics of this paper.

8. References

1. Headquarters Department of the Army, "Fundamentals of Flight," Field Manual (FM) NO. 1-203, US Army Adjutant General Publications Center, September 9, 1983.

2. Tomasic, J. E., Brown, S., "GADGHT Tomorrow's Moving Map Today," GADGHT Team, VH Systems Engineering IPT, June 1999.

3. Varnes, David J., "Development of a Helicopter Vortex Ring State Warning System through a Moving Map Display Counter," Thesis for M.S.A.E. Degree, Naval Postgraduate School, September 1999.

4. Moore, Benjamin H., "Dead Air", *Rotor & Wing*, Volume 33, Number 5, May 1999.

5. Scheiman, James, "A Tabulation of Helicopter Rotor-Blade Differential Pressures, Stresses, and Motions as Measured In Flight," NASA TM X-952, Langley Research Center, Hampton, VA, 691 pages., National Aeronautics and Space

Administration, Washington, D.C. 20230, March 1964.

6. Prouty, Raymond W., Helicopter Performance, Stability, and Control, Krieger Publishing Company, Inc., Malabar, FL, 1995.

7. Gessow, Alfred and Myers, Garry C. Jr., Aerodynamics of the Helicopter, Frederick Ungar Publishing Co., New York, Sixth Printing 1981.

8. Gao, Zheng, and Xin, Hong, "An Experimental Investigation on Vortex-Ring State Boundary," First Russian Helicopter Society Annual Forum Proceedings, August 1994.

9. Wolkovitch, Julian, "Analytical Prediction of Vortex-Ring State Boundaries for Helicopters in Steep Descents," Journal of the American Helicopter Society, July 1972.

10. Peters, David, A., and Chen, Shyi-Yuang, "Momentum Theory, Dynamic Inflow, and the Vortex-Ring State," Journal of the American Helicopter Society, July 1982.

11. Drees, Jan et al., "Flow through a Helicopter Rotor", The Dutch Helicopter Foundation, National Aeronautical Research Institute, Amsterdam, 1950.

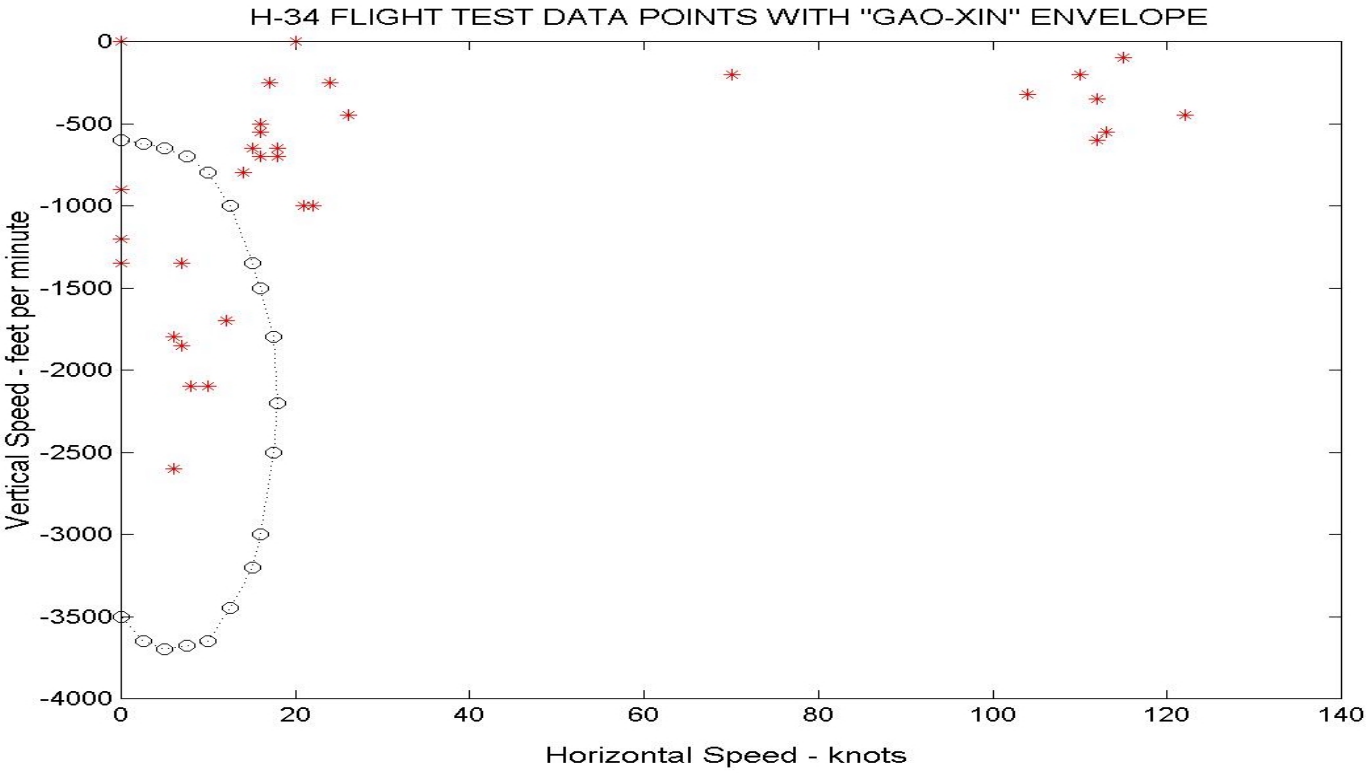

Figure 7. "Gao-Xin Envelope" of Ref. 8 superimposed on NASA partial power descent flight test data points for instrumented Army-Sikorsky H-34 helicopter of Ref. 5.

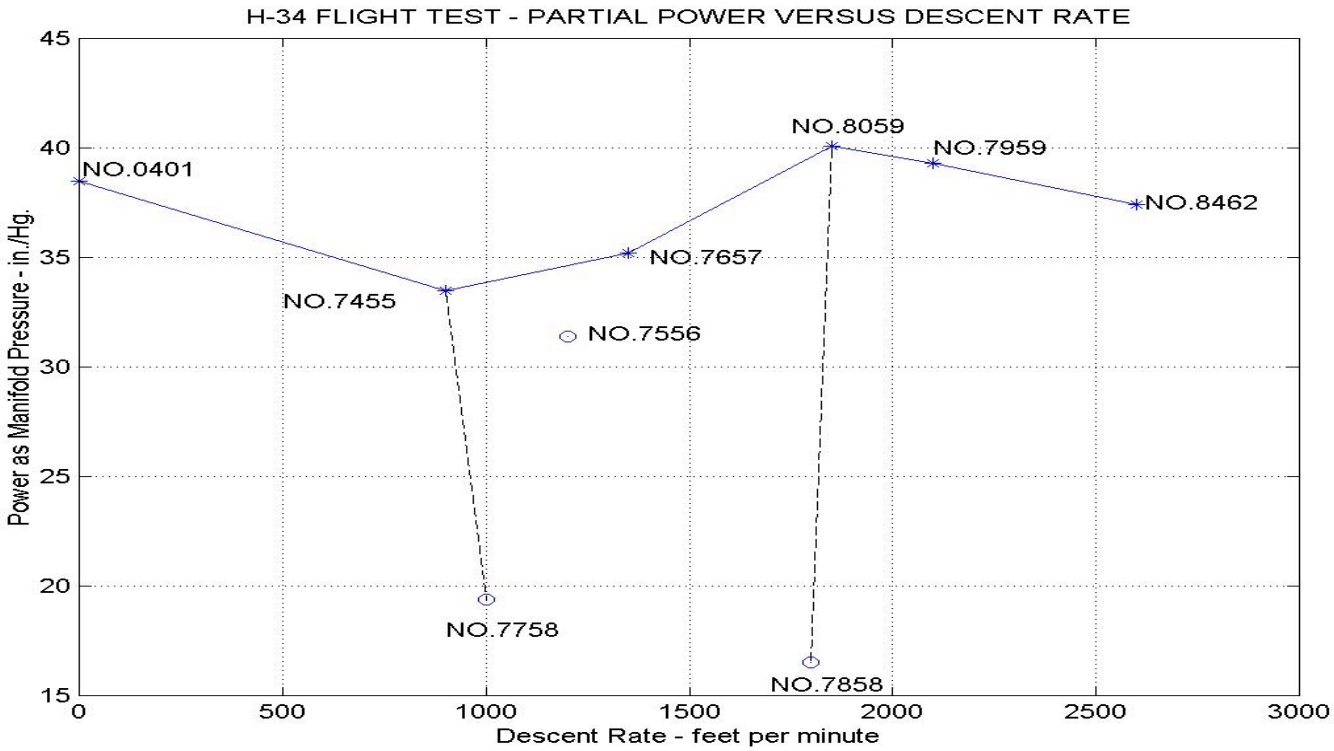

Figure 8. Manifold pressure (in. Hg.) vs descent rate (fpm) for Army-Sikorsky H-34 helicopter in vertical descent. V_H = 1850 fpm. VRS entry at .28V_H is 518 fpm.

TABLE I - H-34 Flight Test Data
NASA TM X-952

Flight	V, knots	Flight Condition	Descent/ Climb Rate (fpm)	Manifold Pressure (in/hg.)	Rotor Speed (rpm)
1	0	Level OGE	Hover	38.5	222
2	11	Level OGE	Hover	40.3	218
5	42	Level OGE	-100	28.0	217
9	68	Level OGE	+120	29.7	194
14	104	Level OGE	-230	42.2	223
17	110	Level OGE	-200	45.3	246
18	112	Level OGE	-350	43.8	216
19	115	Level OGE	-100	46.5	231
20	122	Level OGE	-450	49.4	245
21	13	Level OGE	0	43.1	210
55	0	PP Desc.	-900	33.5	211
56	0	PP Desc.	-1200	31.4	214
57	0	PP Desc.	-1350	35.2	215
58	7	PP Desc.	-1000	19.4	234
58	6	PP Desc.	-1800	16.5	206
59	8	PP Desc.	-2100	39.3	210
59	7	PP Desc.	-1850	40.1	206
60	10	PP Desc.	-800	29.9	211
61	12	PP Desc.	-1700	30.3	223
62	14	PP Desc.	-2000	35.4	225
62	6	PP Desc.	-2600	37.4	218
63	15	PP Desc.	-650	36.2	214
64	16	PP Desc.	-500	28.0	215
65	17	PP Desc	-250	43.4	215
66	16	PP Desc	-550	33.6	215
67	16	PP Desc	-700	40.5	210
68	18	PP Desc	-650	37.2	204
69	18	PP Desc	-700	34.5	222
70	20	PP Desc	0	43.5	211
71	21	PP Desc	-1000	19.7	215
72	22	PP Desc	-1000	18.3	208
73	24	PP Desc	-250	38.9	211
74	26	PP Desc	-450	29.7	225
75	70	PP Desc	-200	28.6	213
76	112	PP Desc	-600	42.2	213
76	113	PP Desc	-550	42.3	213

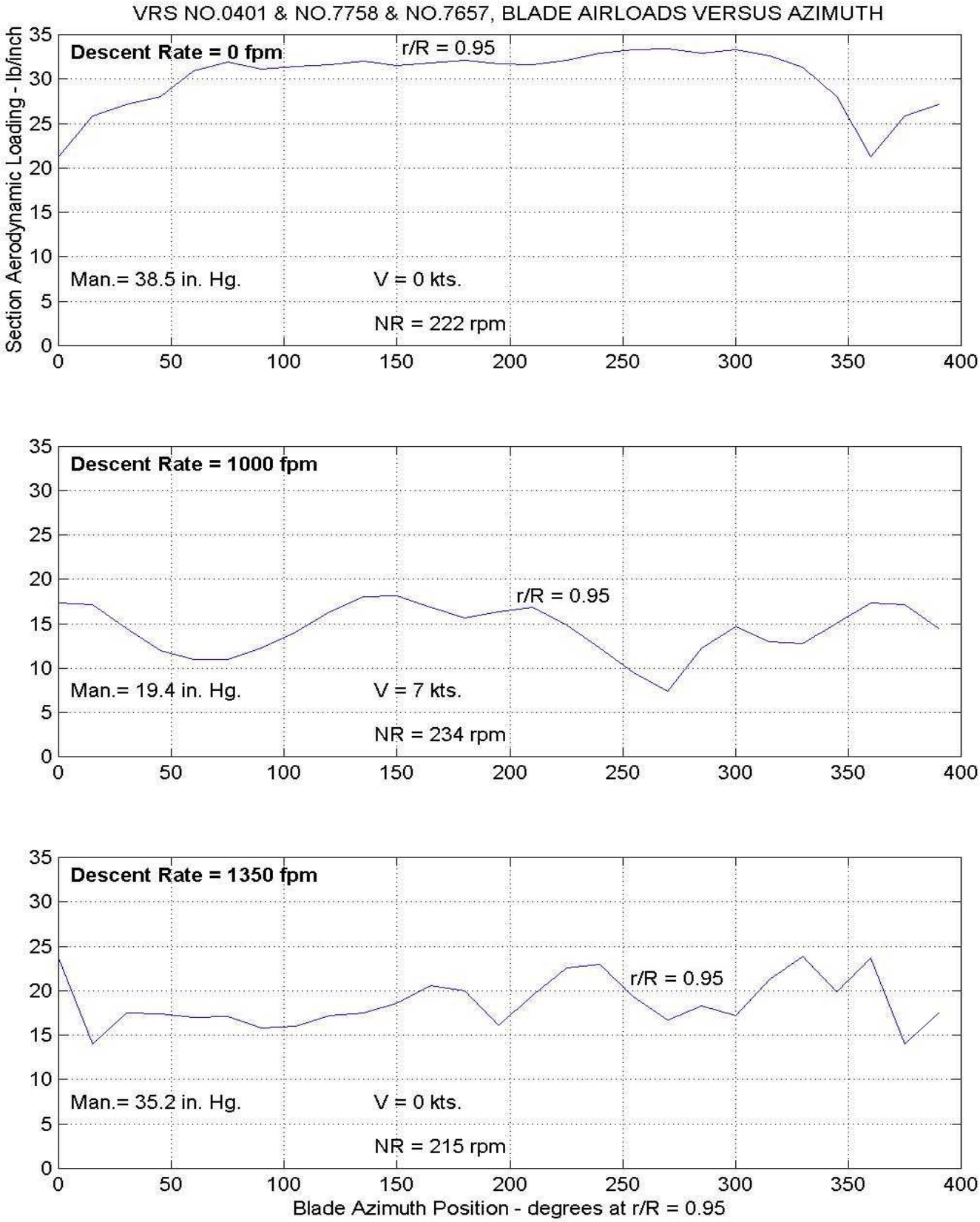

Figure 9. Time history of measured blade airloads in one rotor revolution (.25 secs.) at 95 percent blade span for rates of vertical descent: hover, 1000 fpm and 1350 fpm.

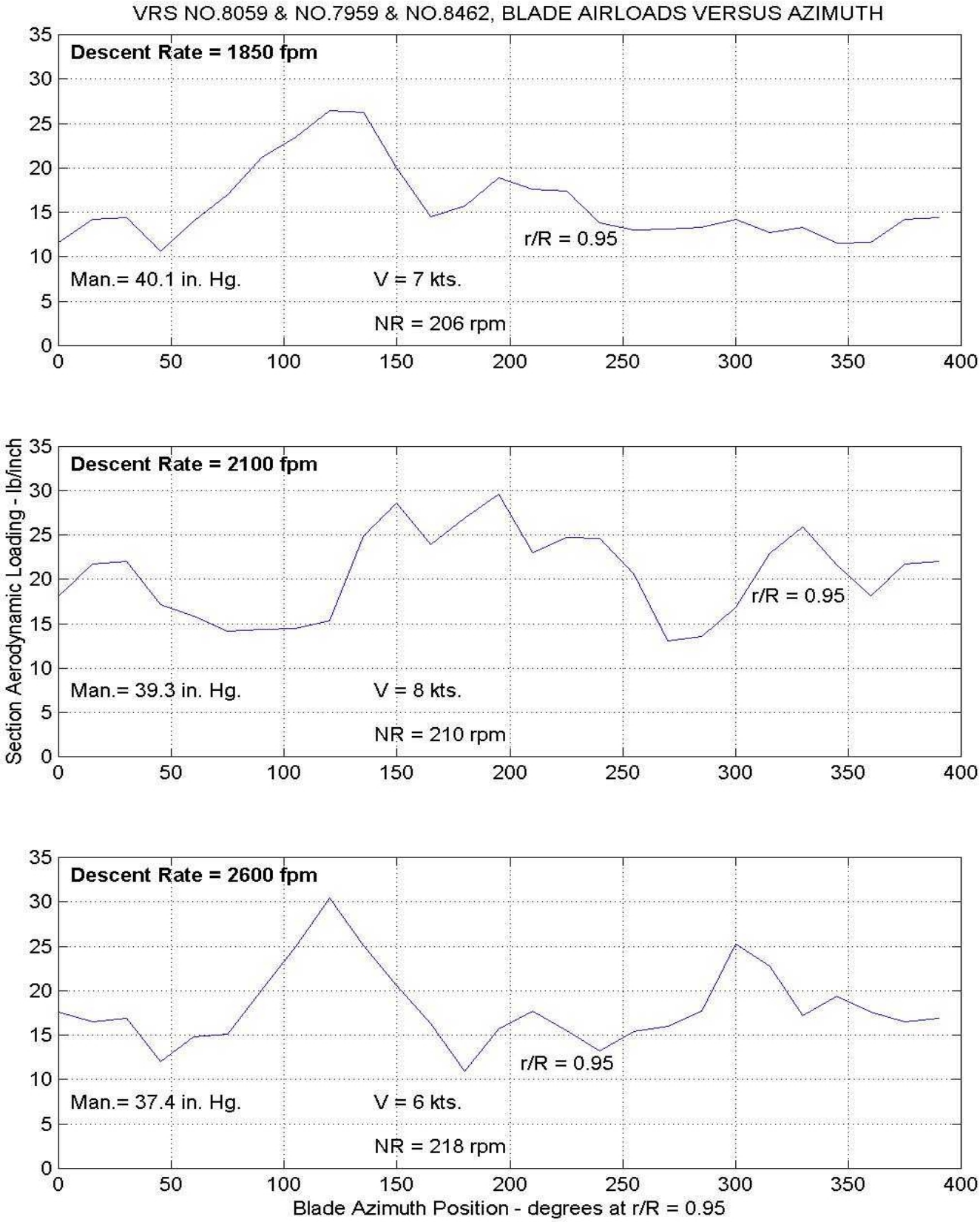

Figure 10. Time history of measured blade airloads in one rotor revolution (.25 secs.) at 95 percent blade span for rates of vertical descent: 1850 fpm, 2100 fpm and 2600 fpm.

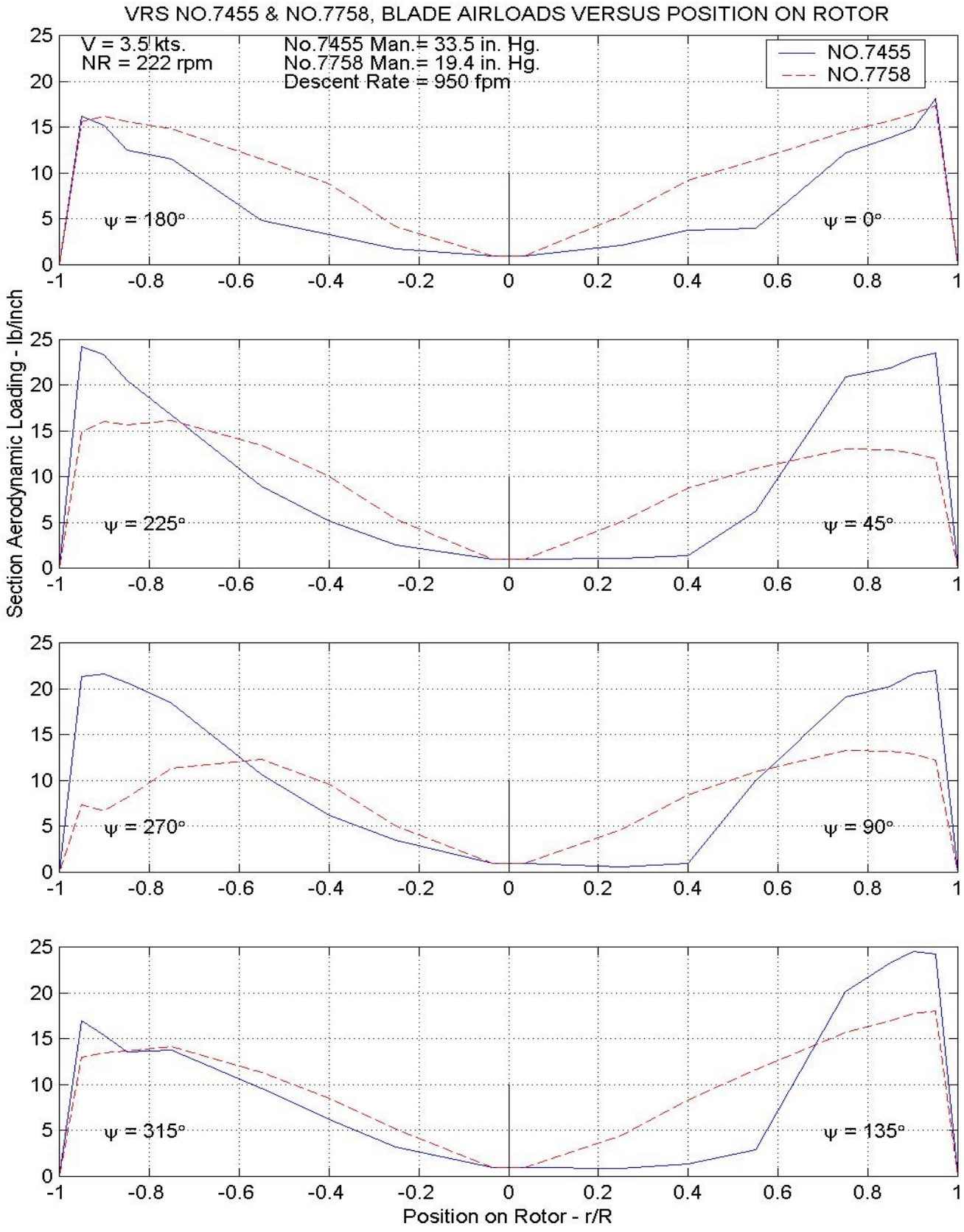

Figure 11. Blade spanwise lift distribution for)Θ = B/4 at 950 fpm descent rate for two equilibrium power settings, one high and one low.

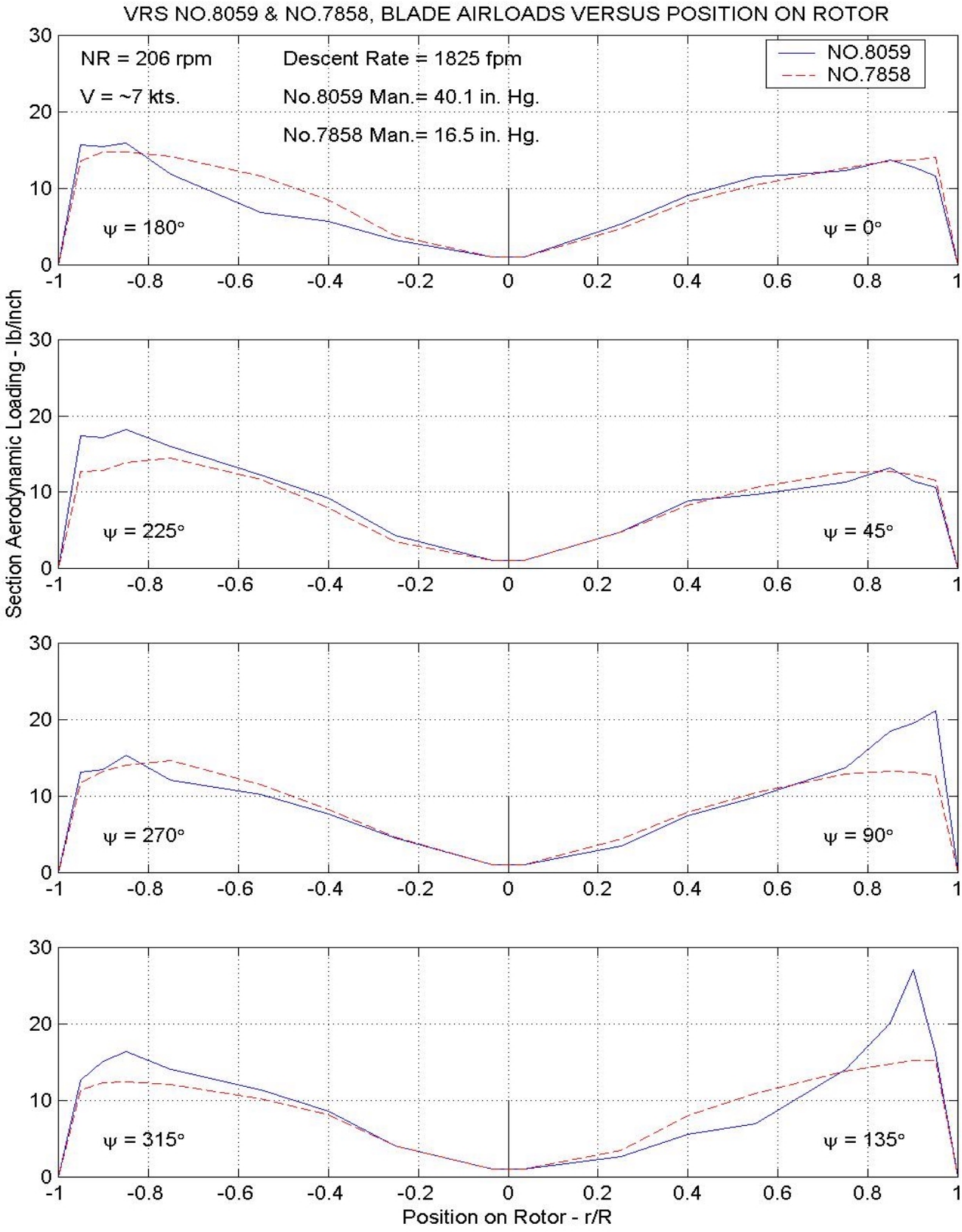

Figure 12. Blade spanwise lift distribution for)Θ = B/4 at 1825 fpm descent rate for two equilibrium power settings, one high and one low.

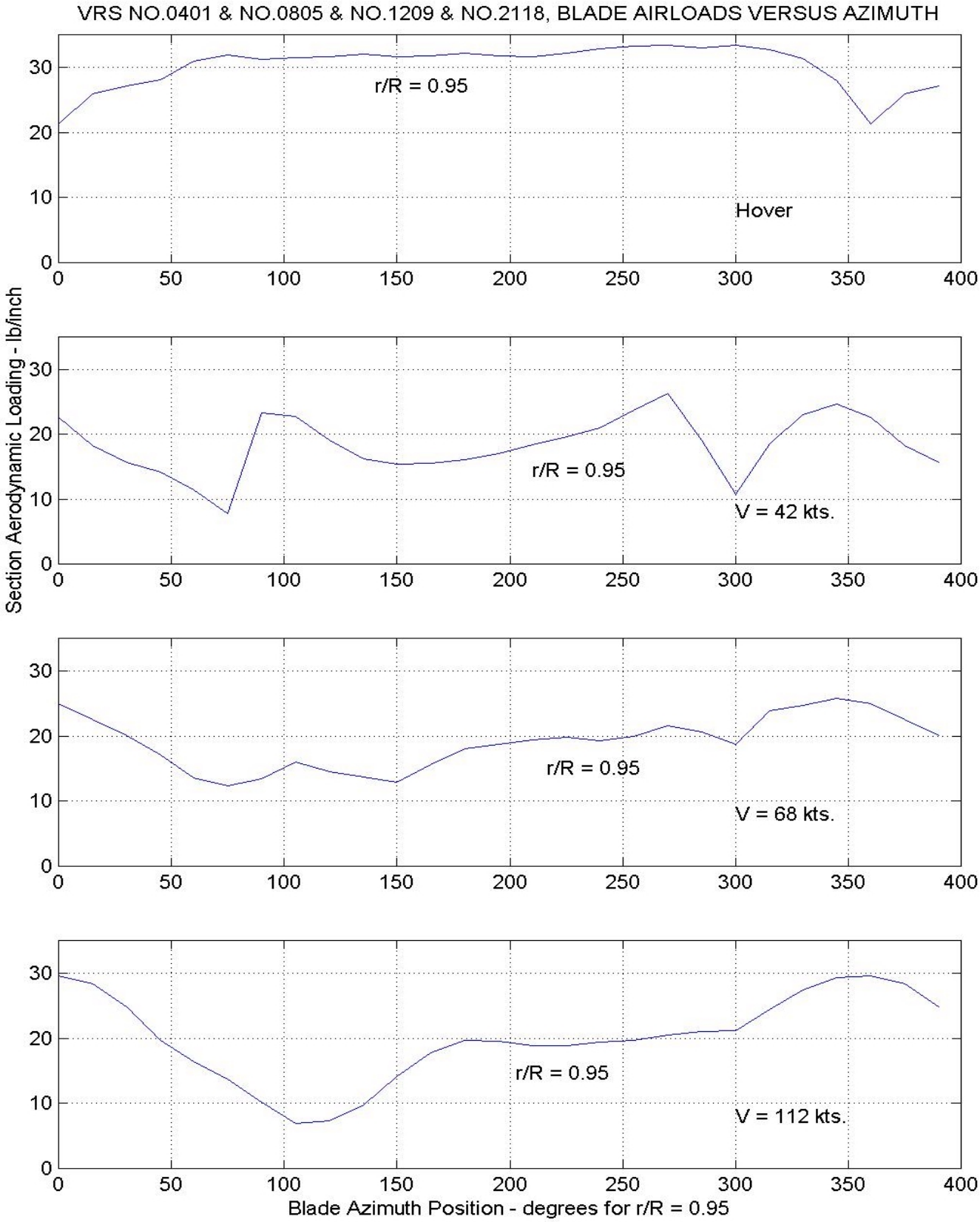

Figure 13. Blade airload at r/R = 95% versus azimuth for four trim and level flight conditions: hover, 42 knots, 68 knots, and 112 knots.

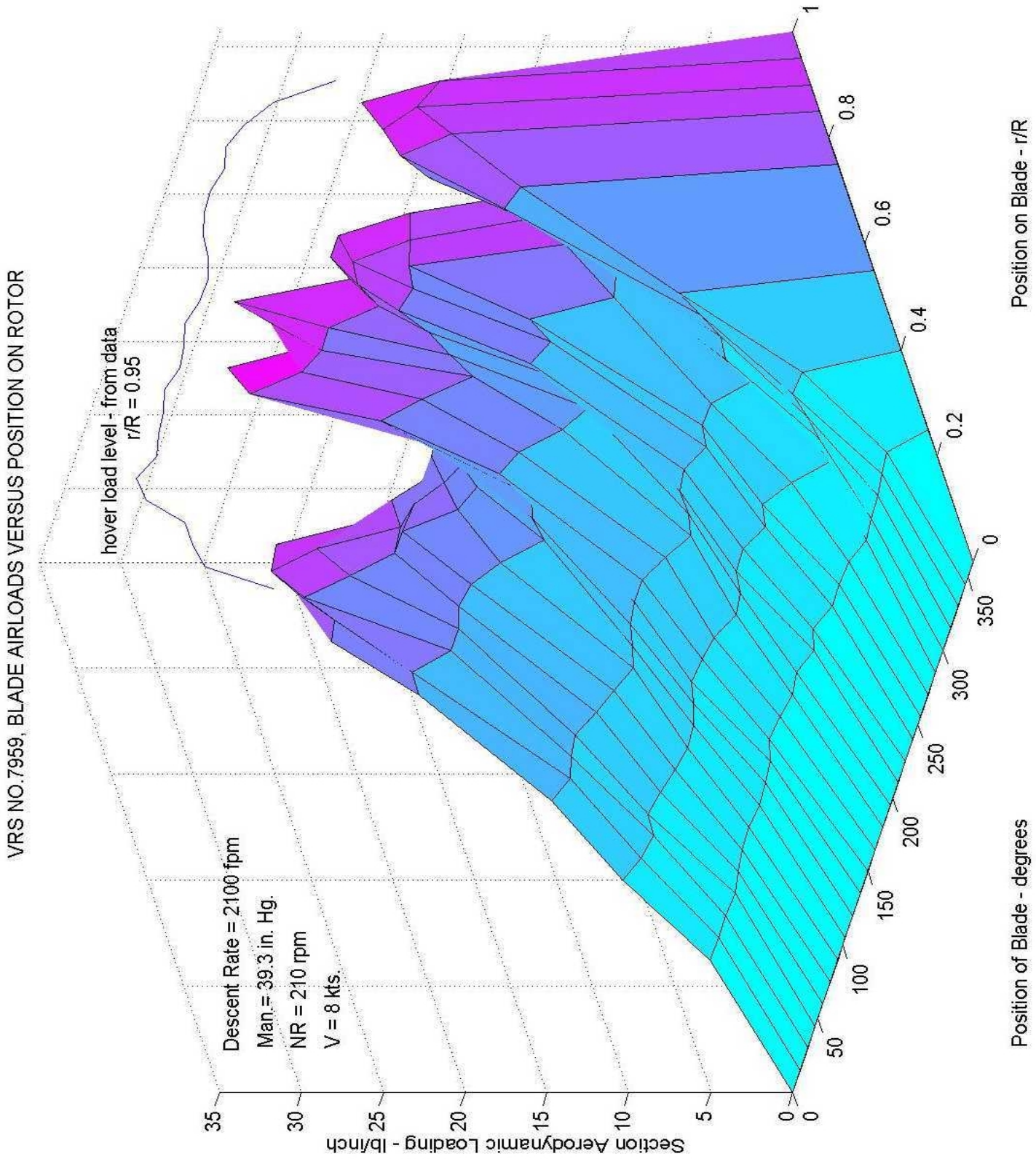

Figure 14. Blade airloads versus azimuth at 2100 fpm rate of descent, showing inflight roughness of typical flight regime in "Vortex-Ring State".